International Journal of Thermophysics, Vol. 10, No. 3, 1989

Measurements of the Vapor–Liquid Coexistence Curve and the Critical Parameters for 1,1,1,2-Tetrafluoroethane[1]

Y. Kabata,[2] S. Tanikawa,[2] M. Uematsu,[2] and K. Watanabe[2]

Measurements of the vapor–liquid coexistence curve in the critical region for 1,1,1,2-tetrafluoroethane (R134a; CH_2FCF_3), which is currently considered as a prospective substitute for conventional refrigerant R12, have been performed by visual observation of the disappearance of the meniscus at the vapor–liquid interface within an optical cell. Twenty-seven saturated densities along the vapor–liquid coexistence curve between 208 and 999 $kg \cdot m^{-3}$ have been obtained in the temperature range 343 K to the critical temperature. The experimental uncertainties in temperature and density measurements have been estimated to be within ± 10 mK and $\pm 0.55\%$, respectively. On the basis of these measurements near the critical point, the critical temperature and the critical density for 1,1,1,2-tetrafluoroethane were determined in consideration of the meniscus disappearing level as well as the intensity of the critical opalescence. In addition, the critical exponent β along the vapor–liquid coexistence curve has been determined in accord with the difference between the density of the saturated liquid and that of the saturated vapor.

KEY WORDS: critical exponent; critical parameter; critical point; 1,1,1,2-tetrafluoroethane; vapor–liquid coexistence curve.

1. INTRODUCTION

In the last several years, the possible ozone depletion due to chlorofluorocarbons (CFCs) has become a very important issue and it is our urgent task to develop harmless CFC alternatives with a lesser ozone depletion

[1] Paper presented at the Tenth Symposium on Thermophysical Properties, June 20–23, 1988, Gaithersburg, Maryland, U.S.A.

[2] Department of Mechanical Engineering, Keio University, 3-14-1 Hiyoshi, Kohoku-ku, Yokohama 223, Japan.

0195-928X/89/0500-0605$06.00/0

potential and greenhouse effect potential. 1,1,1,2-Tetrafluoroethane (R134a; CH_2FCF_3) is proposed as one of the most prospective alternatives [1] to R12, which is currently used worldwide in many commercialized applications. But no information about its thermodynamic properties is available except for a few sets of numerical values prepared by some leading manufacturers [2–4].

We have measured the vapor–liquid coexistence curve in the critical region and the critical parameters for several refrigerants, i.e., R23 [5], R12 [6], R22 [6], R502 [7], R13B1 [8], R114 [9], and R152a [10], by visual observation of the disappearance of the meniscus at the vapor–liquid interface within an optical cell using the apparatus designed originally by Okazaki et al. [5]. The numerical values of the critical parameters for these refrigerants we measured are listed in Table I.

In the present study, measurements of the vapor–liquid coexistence curve for R134a in the critical region have been performed and the critical temperature and the critical density for R134a have been determined precisely for the first time. In addition, the critical exponent β along the vapor–liquid coexistence curve has been determined in accordance with the difference between the density of the saturated liquid and that of the saturated vapor.

2. EXPERIMENTAL APPARATUS AND PROCEDURE

The vapor–liquid coexistence curve in the critical region for R134a has been measured by observing the meniscus disappearance. The experimental apparatus and procedures, described in detail in our previous publications [5, 7, 8], were used in our previous similar measurements of R23 [5], R12 [6], R22 [6], R502 [7], R13B1 [8], R114 [9], and R152a [10]. The

Table I. Our Measured Values of the Critical Parameters for Eight Refrigerants

Refrigerant	T_c (K)	ρ_c (kg · m^{-3})	Ref. No.
R12 (CCl_2F_2)	385.01 ± 0.01	568 ± 3	6
R22 ($CHClF_2$)	369.32 ± 0.01	515 ± 3	6
R23 (CHF_3)	299.01 ± 0.01	529 ± 5	5
R13B1 ($CBrF_3$)	340.08 ± 0.01	764 ± 3	8
R114 ($CClF_2CClF_2$)	418.78 ± 0.02	576 ± 3	9
R134a (CH_2FCF_3)	374.30 ± 0.01	508 ± 3	
R152a (CH_3CHF_2)	386.44 ± 0.01	368 ± 2	10
R502[a]	355.37 ± 0.01	555 ± 3	7

[a] Azeotropic mixture of 48.8 wt% R22 + 51.2 wt% R115 ($CClF_2CF_3$).

main part of the apparatus is composed of three vessels, i.e., an optical cell with two sapphire windows to observe the meniscus behavior of the sample, an expansion vessel, and a supplying vessel. The apparatus is installed in a thermostated bath where silicone oil (Shin-etsu silicone; KF96-50), as the heat transfer medium, is filled and stirred. The bath temperature is controlled automatically within ± 5 mK. The temperature measurements are conducted with a 25-Ω platinum resistance thermometer (Chino Model R 800-1) mounted in the vicinity of the optical cell with an aid of a thermometer bridge (Tinsley Type 5840). The thermometer has been calibrated on IPTS-68 at the National Research Laboratory of Metrology, Tsukuba, Japan. The sample density, which was calculated from the inner volumes of the three vessels used and the mass of the confined sample, could be changed with the aid of an expansion technique [5] in order to measure the saturation temperature successively for a series of densities along the vapor–liquid coexistence curve. The inner volume of the optical cell, the expansion vessel, and the supplying vessel, calibrated using pure water, are 13.487 ± 0.005, 7.592 ± 0.005, and 77.052 ± 0.005 cm^3, respectively. The sample mass was weighed on a chemical balance (Chyo Model C_2-3000) with an uncertainly of 2 mg. The purity of the sample furnished by Asahi Glass Co., Ltd., Tokyo, was either 99.6 or 99.8 wt% R134a.

3. EXPERIMENTAL RESULTS OF THE VAPOR–LIQUID COEXISTENCE CURVE

Twelve measurements for the saturated liquid density and fifteen for the saturated vapor density of R134a have been obtained along the vapor–liquid coexistence curve in the critical region from 343.2 to 373.3 K ($0.92 < T_r$), corresponding to the density range from 208 to 998.6 kg $\cdot$ m^{-3} ($0.4 < \rho_r < 2.0$). The numerical values of the results shown in Fig. 1 are given in Table II. As far as we have surveyed, these results are the first contribution to reveal the thermodynamic properties of R134a experimentally, and they have made clear the shape of the vapor–liquid coexistence curve for R134a in the critical region.

The uncertainty of temperature measurements is estimated to be within 10 mK, while that of each density measurement is estimated to be between 0.08 and 0.55%, as shown in Table II. The critical opalescence has been observed at 10 measurements for densities between 398.6 and 633.0 kg $\cdot$ m^{-3}, which are indicated by asterisk superscripts in Table II and filled circles in Fig. 1. Twenty-three measurements of the present study were performed using 99.8 wt% R134a, while only four measurements, indicated with dagger superscripts in Table II, were obtained using a 99.6 wt% pure

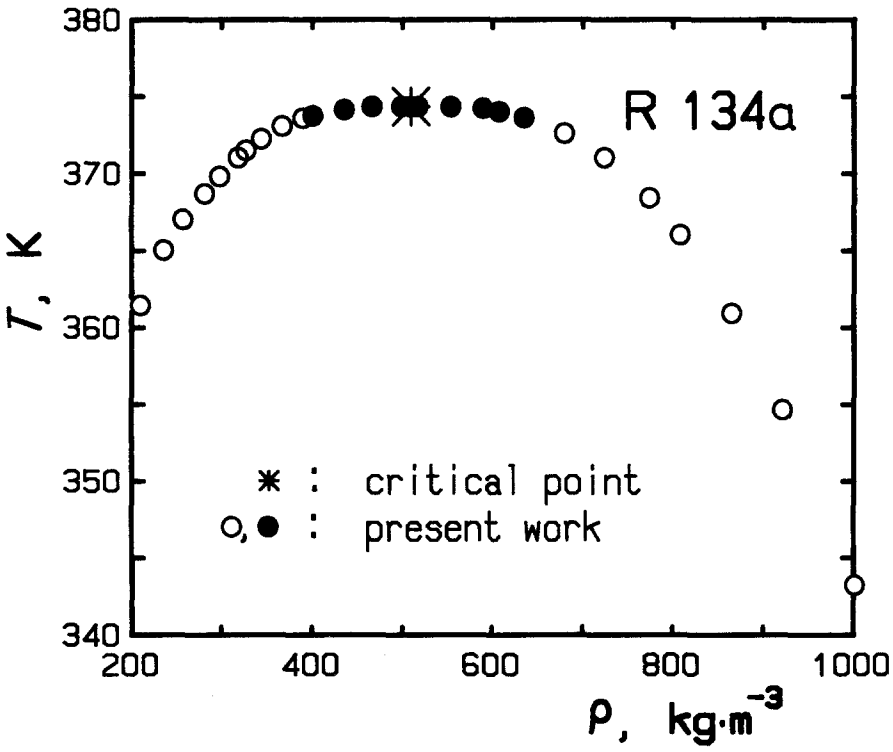

Fig. 1. Experimental results of the vapor–liquid coexistence curve in the critical region for R134a.

sample. We could not find any difference among the present results due to existing differences in sample purity. The meniscus for 13 densities between 207.9 and 464.5 $kg \cdot m^{-3}$ descended with increasing temperatures and disappeared at the bottom of the optical cell, whereas that for 11 densities between 552.2 and 998.6 $kg \cdot m^{-3}$ ascended with increasing temperatures and disappeared at the top of the optical cell. The meniscus for densities of 497.1, 507.5, and 515.6 $kg \cdot m^{-3}$ in the very vicinity of the critical point remained at the center of the optical cell in spite of increasing temperatures, became indistinguishable, and finally disappeared.

4. DETERMINATION OF THE CRITICAL PARAMETERS FOR R134a

The critical point of fluids is defined as the state where all the thermodynamic properties of coexisting vapor and liquid phases become identical.

Table II. Experimental Results for R134a[a]

T (K)	ρ'' (kg · m^{-3})	T (K)	ρ' (kg · m^{-3})
361.42_8	207.9 ± 1.0	374.30_3	515.6 ± 0.4*
365.02_4	233.5 ± 0.8	374.28_8	552.2 ± 1.5*
367.00_9	255.1 ± 0.9	374.18_9	587.9 ± 1.6*
368.67_4	278.7 ± 0.8	373.98_1	605.9 ± 0.9*†
369.78_7	295.5 ± 1.6	373.59_3	633.0 ± 1.0*
371.01_0	316.0 ± 1.5†	372.56_8	677.7 ± 1.0
371.47_2	324.8 ± 0.9	371.00_4	721.6 ± 1.1
372.21_4	341.9 ± 0.5	368.38_0	771.7 ± 0.6†
373.03_1	364.7 ± 0.6	365.98_9	806.4 ± 0.6
373.54_8	387.7 ± 1.4†	360.90_2	863.5 ± 0.7
373.70_4	398.6 ± 0.6*	354.63_8	919.6 ± 0.7
374.10_1	433.6 ± 1.5*	343.22_4	998.6 ± 0.8
374.28_7	464.5 ± 0.4*		
374.30_3	497.1 ± 1.2*		
374.30_1	507.5 ± 0.4*		

[a] Values with an asterisk superscript were measured by observing the critical opalescence. Values with a dagger superscript were measured on a 99.6 wt % pure sample. Values without a dagger measured on a 99.8 wt % pure sample.

That is, the meniscus disappears at the center of the optical cell and the critical opalescence is observed most intensely and equally in both vapor and liquid phases. Based on our measurements we determined the critical temperature and the critical density for R134a in consideration of the meniscus disappearing level as well as the intensity of the critical opalescence.

Figure 2 shows the meniscus behavior for a density of 507.5 kg · m^{-3} throughout the determination of the meniscus disappearing temperature. The ordinate in Fig. 2 is the observed temperature difference from the meniscus disappearing temperature in millikelvins and the abscissa is the elapsed time from the first observation of the meniscus in hours. For this density the meniscus existed at the center of the cell with increasing temperatures and the critical opalescence was observed first at a temperature of about 200 mK below the temperature at which the meniscus disappeared. According to the intensity of the critical opalescence, we reduced the rate of the temperature increase gradually. Approaching the meniscus disappearing temperature, the meniscus became indistinguishable so that it was essential to keep the temperature constant over 1 to 10 h while the meniscus behavior was carefully observed. Then the bath temperature was increased by 5 mK, and the observation was continued. Repeating this procedure until the meniscus disappeared completely, the saturation tem-

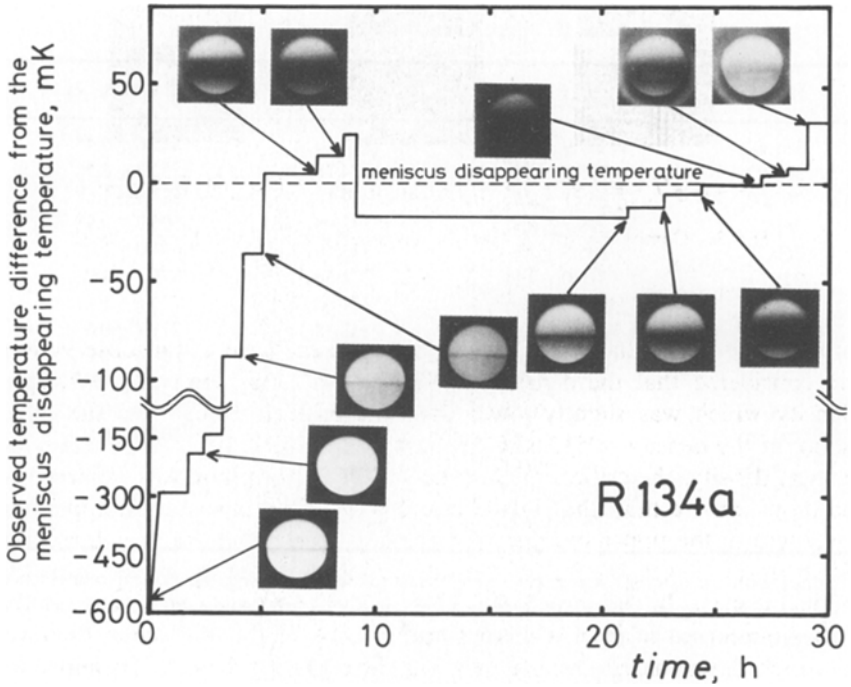

Fig. 2. Observation of the meniscus level and the critical opalescence at various temperatures as a function of time at a density of 507.5 $kg \cdot m^{-3}$.

perature was determined as the temperature when the vapor–liquid interface disappeared. In the case of this density, the observation of meniscus behavior was repeated twice around the meniscus disappearing temperature within ± 20 mK as shown in Fig. 2. We could observe the critical opalescence most intensely at 374.30 K, which was determined as the temperature when the vapor–liquid interface disappeared. The level at which the meniscus disappeared was the center of the optical cell. It takes over 30 h to determine the meniscus disappearing temperature for the density 507.5 $kg \cdot m^{-3}$, which was closest to the critical density.

For three different densities of, 497.1, 507.5 (mentioned above), and 515.6 $kg \cdot m^{-3}$, a comparison of the meniscus disappearing level and the intensity of the critical opalescence is shown in Fig. 3 with the aid of photos of the observed meniscus at the meniscus disappearing temperature for each experimental density. These measurements have been performed for densities within 20 $kg \cdot m^{-3}$ in difference across the critical density. At the density of 497.1 $kg \cdot m^{-3}$, which is about 2.1% lower than the critical density, the level at which the meniscus disappeared was in the lower quarter. The critical opalescence in the liquid phase was observed to be

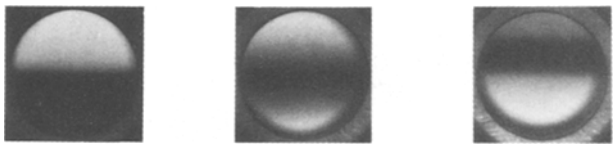

Fig. 3. Comparison of the meniscus disappearing level and the intensity of the critical opalescence at the meniscus disappearing temperature for densities of 497.1, 507.5, and 515.6 $kg \cdot m^{-3}$.

more intense than that in the vapor phase. On the basis of this observation, we considered that the density of 497.1 $kg \cdot m^{-3}$ was the saturated vapor density which was slightly lower than the critical density. On the other hand, at the density of 515.6 $kg \cdot m^{-3}$, which is about 1.5% larger than the critical density, the critical opalescence in the vapor phase was observed to be more intense than that in the liquid phase. The meniscus disappearing level was in the upper quarter. Therefore we concluded that the density of 515.6 $kg \cdot m^{-3}$ was the liquid density which was slightly higher than the critical density. In the case of 507.5 $kg \cdot m^{-3}$, the critical opalescence in the vapor phase was as intense as that in the liquid phase. Moreover, the level at which the meniscus disappeared was the center of the cell. Therefore we considered that the density of 507.5 $kg \cdot m^{-3}$ was the density closest to the critical density among these measurements.

In consideration of the meniscus behavior with respect to the three densities mentioned above, the critical density of R134a was determined, finally, as

$$\rho_c = 508 \pm 3 \text{ kg} \cdot \text{m}^{-3}$$

The critical temperature T_c can be determined as the saturation temperature along the vapor–liquid coexistence curve corresponding to the critical density. As shown in Table II, the temperatures at which the meniscus disappeared for five measurements near the critical point in the

Table III. Reported Values of the Critical Parameters for R134a

Investigator	Year	T_c (K)	ρ_c ($kg \cdot m^{-3}$)	Sample purity (wt%)
du Pont [2]	1979	373.69	495.6	
ICI [3]	1987	379.6_5	512.25	
Allied-Signal [4]	1987	374.2_6	517	
Present work	1988	374.30 ± 0.01	508 ± 3	99.6 or 99.8

density range between 464.5 and 552.2 $kg \cdot m^{-3}$ agree with each other within estimated uncertainties of the temperature measurements. The temperature for the density of 507.5 $kg \cdot m^{-3}$, closest to the critical density, was measured as 374.301 K. Therefore, the critical temperature of R134a was determined as

$$T_c = 374.30 \pm 0.01 \text{ K}$$

The available information about the critical parameters of R134a has been reported recently by three sources, i.e., du Pont [2], ICI [3], and Allied-Signal [4], as summarized in Table III. Since those values appeared in nonscientific publications, how to obtain these values with associated uncertainties has not been reported. The present T_c value is in good agreement with the value of Allied-Signal. But it is lower than that of du Pont by 0.61 K and higher than that of ICI by 5.3 K. With respect to the critical density, the present value is in good agreement with that of ICI. But it is larger than that of du Pont by a density deviation of 2.4% and smaller than that of Allied-Signal by a deviation of 1.8%.

5. THE CRITICAL EXPONENT β ALONG THE COEXISTENCE CURVE

The critical exponent β along the coexistence curve is important to represent the vapor–liquid coexistence curve in the critical region and can be defined by a simple power-law representation,

$$(\rho' - \rho'')/2\rho_c = B|(T - T_c)/T_c|^{\beta} \tag{1}$$

where ρ', ρ'', T, ρ_c, T_c, and B denote the saturated liquid and vapor densities in the coexisting condition, the temperature, the critical density, the critical temperature, and an adjustable parameter, respectively. In the present study, it is impossible to measure the densities of the saturated liquid and vapor at a common temperature. Therefore we represented the vapor–liquid coexistence curve in the critical region based on the present measurements and correlated the coexisting densities corresponding to the present data for the saturated vapor or liquid densities. Then the critical exponent β can be determined by Eq. (1).

With respect to the correlation of the vapor–liquid coexistence curve in the critical region, we have correlated the following expression, which is a combination of two representations for the coexistence curve by Wegner expansion [11] in conjunction with the scaling laws as reported in our previous papers for R114 [9] and R152a [10].

$$\Delta\rho^* = 6.44134\,|\Delta T^*|^{0.8915} - 9.07748\,|\Delta T^*| + 4.28364\,|\Delta T^*|^{1.3915} \pm 1.8035\,|\Delta T^*|^{0.325} \pm 0.641723\,|\Delta T^*|^{0.825} \tag{2}$$

where $\Delta\rho^* = (\rho - \rho_c)/\rho_c$ and $\Delta T^* = (T - T_c)/T_c$. The upper (plus) sign of the fourth and fifth terms in Eq. (2) corresponds to the saturated liquid, and the lower (minus) sign to the saturated vapor. The critical density ρ_c and the critical temperature T_c of Eq. (2) correspond to the present values determined in Section 4. Twenty-one present data were used as the input data for correlating the vapor–liquid coexistence curve for R134a, except for six measurements of densities between 464.5 and 587.9 $kg \cdot m^{-3}$ in the very vicinity of the critical point. The numerical values of coefficients in Eq. (2) were determined by least-squares fitting. Equation (2) reproduces 9 present liquid densities used as the input data with an average deviation of 0.09% and 12 present vapor densities with 0.55%, respectively.

Figure 4 shows the logarithmic relation between $(\rho' - \rho'')/2\rho_c$ and $(T - T_c)/T_c$ depicted in term of the present measurements and calculated results by Eq. (2). Circles correspond to results based on the experimental liquid densities, and squares to those based on the experimental vapor densities. The power-law representation by Eq. (1) suggests that the experimental results may be fitted satisfactorily by a straight line with a gradient equivalent to the critical exponent β in a plot such as shown in Fig. 4. Nineteen data in the range of the reduced temperature difference $5.3 \times 10^{-4} < |(T - T_c)/T_c| < 3.5 \times 10^{-2}$ were available for determination of the critical exponent β. Six measured densities in the very vicinity of the critical point and two saturated liquid densities in the lower temperature

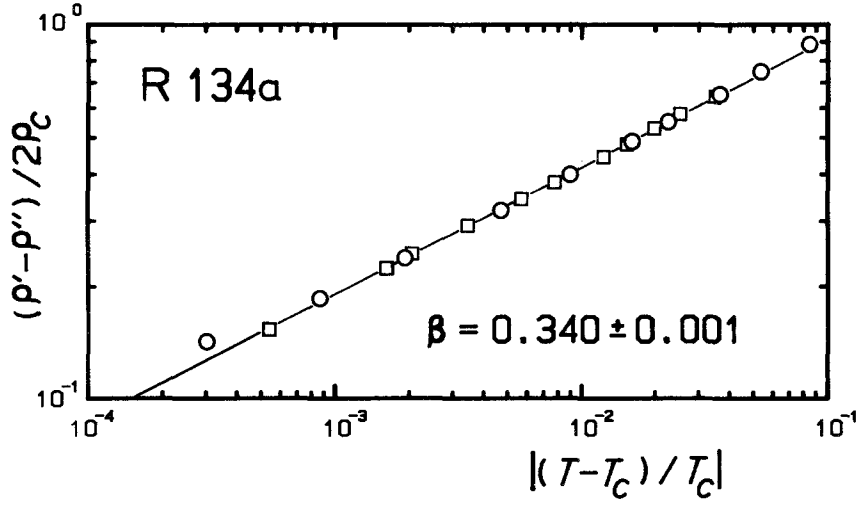

Fig. 4. Relation between $(\rho' - \rho'')/2\rho_c$ and $|(T - T_c)/T_c|$.

range, below 360 K, were excluded from the input data. As a result of least-squares fitting, the values of β and B were obtained as follows:

$$\beta = 0.340 \pm 0.001$$

$$B = 2.009 \pm 0.014$$

Equation (2) was correlated with slightly large deviations in the lower density region, i.e., 1.4% for 207.9 $kg \cdot m^{-3}$ and -1.3% for 233.5 $kg \cdot m^{-3}$, but no significant difference was found between the value of β mentioned above and that calculated due to respective correlations independently developed for either the vapor or the liquid densities.

In the case of R134a, the value of the exponent β seems to be little greater than the theoretical value of 0.325 due to scaling-law analysis [11]. It is also noteworthy that the present β value indicates a good agreement with the exponent $\beta = 0.337$ which was determined as being an averaged value for six refrigerants, i.e., $\beta = 0.329$ for R12 [12], 0.345 for R22 [12], 0.344 for R23 [12], 0.343 for R13B1 [12], 0.328 for R114 [12], and 0.333 for R152a [13], respectively.

6. CONCLUSION

In the present study, we measured the vapor–liquid coexistence curve of 1, 1, 1, 2-tetrafluoroethane (R134a) in the critical region for the first time and made clear its shape on the T–ρ plane. On the basis of the present data near the critical point, we determined the critical temperature and the critical density for R134a with a high accuracy. We believe that the present results are very useful so as to construct the thermodynamic state surface of this important CFC alternative for the future. In addition, the critical exponent β along the vapor–liquid coexistence curve was determined in accordance with the difference between the density of the saturated liquid and that of the saturated vapor.

ACKNOWLEDGMENTS

The authors are greatly indebted to Asahi Glass Co., Ltd., Tokyo, for kindly furnishing the sample, to the National Research Laboratory of Metrology, Tsukuba, Japan, for the calibration of the thermometer, and to Shin-etsu Chemicals Co., Ltd., Tokyo, for kindly furnishing the silicone oil.

REFERENCES

1. E. I. du Pont de Nemours & Co., *UPDATE Fluorocarbon/Ozone* (June 1980).
2. E. I. du Pont de Nemours & Co. (1979).

3. ICI Chemical & Polymers, ARCTON 134a preliminary data sheet (1987).
4. Allied-Signal Inc., *Fluorocarbons for tomorrow* (1987).
5. S. Okazaki, Y. Higashi, Y. Takaishi, M. Uematsu, and K. Watanabe, *Rev. Sci. Instrum.* **54**:21 (1983).
6. Y. Higashi, S. Okazaki, Y. Takaishi, M. Uematsu, and K. Watanabe, *J. Chem. Eng. Data* **29**:31 (1984).
7. Y. Higashi, M. Uematsu, and K. Watanabe, *Int. J. Thermophys.* **5**:117 (1984).
8. Y. Higashi, M. Uematsu, and K. Watanabe, *Bull. JSME* **28**:2660 (1985).
9. Y. Higashi, M. Uematsu, and K. Watanabe, *Bull. JSME* **28**:2969 (1985).
10. Y. Higashi, M. Ashizawa, Y. Kabata, T. Majima, M. Uematsu, and K. Watanabe, *JSME Int. J.* **30**:1106 (1987).
11. J. M. H. Levelt Sengers and J. V. Sengers, in *Perspectives in Statistical Physics*, H. J. Raveché, ed. (North-Holland, Amsterdam, 1981), Chap. 14.
12. Y. Higashi, Ph.D. thesis (Keio University, Yokohama, Japan, 1986).
13. Y. Kabata, B.S. thesis (Keio University, Yokohama, Japan, 1986).